Clinical Cancer Research

Survival and Proliferation of Neural Progenitor–Derived Glioblastomas Under Hypoxic Stress is Controlled by a CXCL12/CXCR4 Autocrine-Positive Feedback Mechanism

Anda-Alexandra Calinescu[1], Viveka Nand Yadav[1], Erica Carballo[1], Padma Kadiyala[1], Dustin Tran[1], Daniel B. Zamler[1], Robert Doherty[1], Maithreyi Srikanth[1], Pedro Ricardo Lowenstein[1,2], and Maria Graciela Castro[1,2]

Abstract

Purpose: One likely cause of treatment failure in glioblastoma is the persistence of glioma stem-like cells (GSLCs) which are highly resistant to therapies currently employed. We found that CXCL12 has highest expression in glioma cells derived from neural progenitor cells (NPC). The development and molecular signature of NPC-derived glioblastomas were analyzed and the therapeutic effect of blocking CXCL12 was tested.

Experimental Design: Tumors were induced by injecting DNA into the lateral ventricle of neonatal mice, using the Sleeping Beauty transposase method. Histology and expression of GSLC markers were analyzed during disease progression. Survival upon treatment with pharmacologic (plerixafor) or genetic inhibition of CXCR4 was analyzed. Primary neurospheres were generated and analyzed for proliferation, apoptosis, and expression of proteins regulating survival and cell-cycle progression.

Results: Tumors induced from NPCs display histologic features of human glioblastoma and express markers of GSLC. *In vivo*, inhibiting the CXCL12/CXCR4 signaling axis results in increased survival of tumor-bearing animals. *In vitro*, CXCR4 blockade induces apoptosis and inhibits cell-cycle progression, downregulates molecules regulating survival and proliferation, and also blocks the hypoxic induction of HIF-1α and CXCL12. Exogenous administration of CXCL12 rescues the drug-induced decrease in proliferation.

Conclusions: This study demonstrates that the CXCL12/CXCR4 axis operates in glioblastoma cells under hypoxic stress via an autocrine-positive feedback mechanism, which promotes survival and cell-cycle progression. Our study brings new mechanistic insight and encourages further exploration of the use of drugs blocking CXCL12 as adjuvant agents to target hypoxia-induced glioblastoma progression, prevent resistance to treatment, and recurrence of the disease. *Clin Cancer Res; 23(5); 1250–62. ©2016 AACR.*

Introduction

Major questions in the pathogenesis of glioblastoma include the identity of the cell-of-origin (1, 2) therapeutic targeting of glioma stem-like cells (GSLC), which are resistant to chemo- and radiotherapy (3), responsible for promoting tumor vasculature (4, 5) and disease recurrence. Accumulating data support three possible cellular origins for glioblastoma: astrocytes, neural stem cells (NSC), and oligodendrocyte precursors (2, 6). The hierarchical relationship between the cell(s) of origin and GSLCs is still unknown. Nonetheless, GSLCs share many characteristics of NSCs (7), including high proliferative potential, association with blood vessels, telomerase activity (8, 9), high motility, diversity of progeny, and similar expression profiles: Nestin, CD133 (10), Olig2 (11), integrin-α6, CD15 (SSEA), L1CAM, A2B5, and Sox2.

In the postnatal mammalian brain, the largest pool of NSCs is present in the subventricular zone (SVZ) of the lateral ventricles and is represented by B cells, radial glia-like cells with astrocyte characteristics, giving rise to rapidly dividing intermediate progenitor cells (C cells), which generate migrating neuroblasts (A cells; ref. 12; Fig. 1A). A subset of B cells communicates directly with the CSF via a unique cillium (13), which passes medially in between ependymal cells. B cells extend a long process laterally, making contact with the vasculature of the SVZ (14). Within the tumor, GSLCs are found in specialized hypoxic microenvironments in close proximity to blood vessels or regions of necrosis, in which they proliferate and induce the formation of new blood vessels (15). Within the SVZ there is high expression of CXCL12 (16). In the context of glioblastoma, CXCL12 is secreted in response to hypoxic stimuli (17) and localizes in regions of necrosis and proliferating microvessels (18). Hypoxia promotes proliferation and maintenance of GSLCs (19, 20) through induction of HIF1-α, which has also been shown to induce CXCL12 (17). CXCL12 is thus a chemokine present in the NSC as well as in the GSLC niche where it may regulate common features of both GSLCs and NSCs.

[1]Department of Neurosurgery, University of Michigan Medical School, Ann Arbor, Michigan. [2]Department of Cell and Developmental Biology, University of Michigan Medical School, Ann Arbor, Michigan.

Note: Supplementary data for this article are available at Clinical Cancer Research Online (http://clincancerres.aacrjournals.org/).

Corresponding Author: Maria Graciela Castro, Department of Neurosurgery, Department of Cell and Developmental Biology, University of Michigan Medical School, 1150 W. Medical Center Drive, MSRB II, Room 4570, Ann Arbor, MI 48109-5689. Phone: 734-764-7052; Fax: 734-764-7051; E-mail:mariacas@med.umich.edu

doi: 10.1158/1078-0432.CCR-15-2888

Translational Relevance

Treatment failure in glioblastoma patients is thought to be due to the heterogeneous nature of the disease, the presence of the blood–brain barrier, the lack of efficacious targeted chemotherapeutics, and the persistence of glioma stem-like cells (GSLC). This study demonstrates that in neural progenitor cell–derived glioblastoma cells under hypoxic conditions, CXCL12/CXCR4 signaling elicits an autocrine-positive feedback mechanism, which promotes survival and cell-cycle progression. Our study brings new mechanistic insights which warrant the use of drugs blocking CXCL12 as adjuvant agents to target hypoxia-induced glioblastoma progression, prevent resistance to treatment, and recurrence of the disease.

CXCL12 and its cognate signaling receptor, CXCR4, were first identified as regulators of hematopoiesis and lymphocyte trafficking (21) and also have critical roles in CNS development (22, 23). The CXCL12/CXCR4 axis modulates numerous physiologic and pathologic processes and promotes the survival, growth, and metastasis of various cancers (24). In preclinical models of glioblastoma, CXCR4 blockade has been shown to inhibit the growth of some human xenografts (25), to be responsible for neovascularization following radiation (26) and to promote migration of human GSLCs towards the SVZ (16), emphasizing the role of the CXCR4 receptor in glioma progression. Expression of CXCR4 is elevated in human high-grade glioma, correlates with a more invasive phenotype of the disease and worse prognosis (27, 28). Levels of CXCR4 are also enhanced in human $CD133^+$ GSLCs (29).

In a microarray screen of several glioma cells, we identified CXCL12 to have highest expression in glioblastoma cells derived from the malignant transformation of NPCs from the SVZ. In this study, we demonstrate that NPC-derived glioblastomas recapitulate the histologic features of human glioblastoma, express CXCL12, markers of GSLCs and respond to treatment with the CXCR4 inhibitor plerixafor, which increases survival of tumor-bearing animals. *In vitro*, plerixafor induces apoptosis and decreases cell-cycle progression of GSLCs through a CXCL12-dependent autocrine-positive feedback mechanism acting upon proteins downstream of several critical glioblastoma signaling pathways regulating survival (pAkt, Bcl-XL) and cell-cycle progression (Cyclin D1, cdk4/cdk6). Importantly, we show that plerixafor inhibits the hypoxic induction of HIF-1α, in both mouse and human glioblastoma cells. HIF-1α plays a pivotal role in the maintenance of normal NSCs and cancer stem-like cells, induction of tumor angiogenesis, genomic instability, metabolic shift, survival, migration, and metastasis (30). We propose that blocking the CXCL12 pathway can be therapeutically beneficial to target hypoxia-induced glioblastoma progression.

Materials and Methods

Animals, generation of NPC-derived tumors and analysis by histology, and IHC

All animal protocols were approved by the University of Michigan Committee of Use and Care of Animals. NPC-derived tumors were generated and characterized by histology and IHC as described previously (31) and elaborated in the Supplementary Methods. *In vivo* treatment with AMD3100 is detailed in the Supplementary Methods.

Glioblastoma cell lines

M7 (NRAS, SV-40LgT) and OL61 (shp53/PDGFB/NRAS) were a gift from Dr. John Ohlfest, Department of Pediatrics, University of Minnesota (3); they were not further authenticated by us. U87MG cells (ATCC HTB-14) were purchased from ATCC and were not further authenticated by us. U251 cells were a gift from Dr. John L. Darling, Institute of Neurology (London, England); they have not been further authenticated by us. HF2303 cells were provided by Dr. Tom Mikkelsen (ref. 7; Department of Neurology, Henry Ford Hospital, Detroit, MI) and were not further authenticated by us. M1, M4, M5 were generated as described previously (2) with NRAS and SV-40 LgT, characterized in this article and were not further authenticated by us. Culture conditions are detailed in the Supplementary Methods.

In vitro analysis of apoptosis, proliferation, and cell-cycle progression, Western blot analysis, and quantitative real-time PCR

In vitro analysis of apoptosis, proliferation, and cell-cycle progression, Western blot analysis, and quantitative real-time PCR were performed using standard methods. Experimental details, antibodies, and primers used are presented in the Supplementary Methods.

Statistical analysis

Statistical analysis was performed using GraphPad Software with either ANOVA or *t* test as specified in the figure legends. Kaplan–Meier survival curves were analyzed using the Mantel–Cox log-rank test.

Results

Gliomas induced by transforming NPCs in neonatal mice with oncogenic DNA express markers characteristic of NSCs and GSLCs

The SVZ of the postnatal mammalian brain is the home of a population of NSCs, which continue to proliferate and generate new neurons, astrocytes and oligodendrocytes throughout life (12, 32). NSCs give rise to intermediate progenitor cells (type C), a subset of which expresses bHLH, a transcription factor for Olig2. Expression of Olig2 is prominent in oligodendrogliomas and also in glioblastoma (33). Olig2 regulates proliferation of NPCs and of $CD133^+$ GSCs (11). We made use of the proliferating capacity of NSCs and of the Sleeping Beauty transposase system (31, 34) to generate endogenous glioblastomas by injecting oncogenic DNA (NRAS and SV40-LgT) into the lateral ventricle of one day old (P1) $CXCL12^{dsRed}$ knock-in mice (35), which express dsRed under the control of the CXCL12 promoter, and analyzed the expression of CXCL12, Nestin, GFAP, and Olig 2 over the course of tumor progression. Ten days after injection (10 days postinjection; dpi), transformed cells, identified by expression of SV-40 Large-T (LgT), are present as small proliferating clusters in regions bordering the lateral ventricles (Fig. 1) associated (Fig. 1D) or not (Fig. 1C) with blood vessels expressing CXCL12. These cells express Nestin (Fig. 1N–P) as well as GFAP (Fig. 1K–M) and Olig2 (Fig. 1H–J) and some cells,

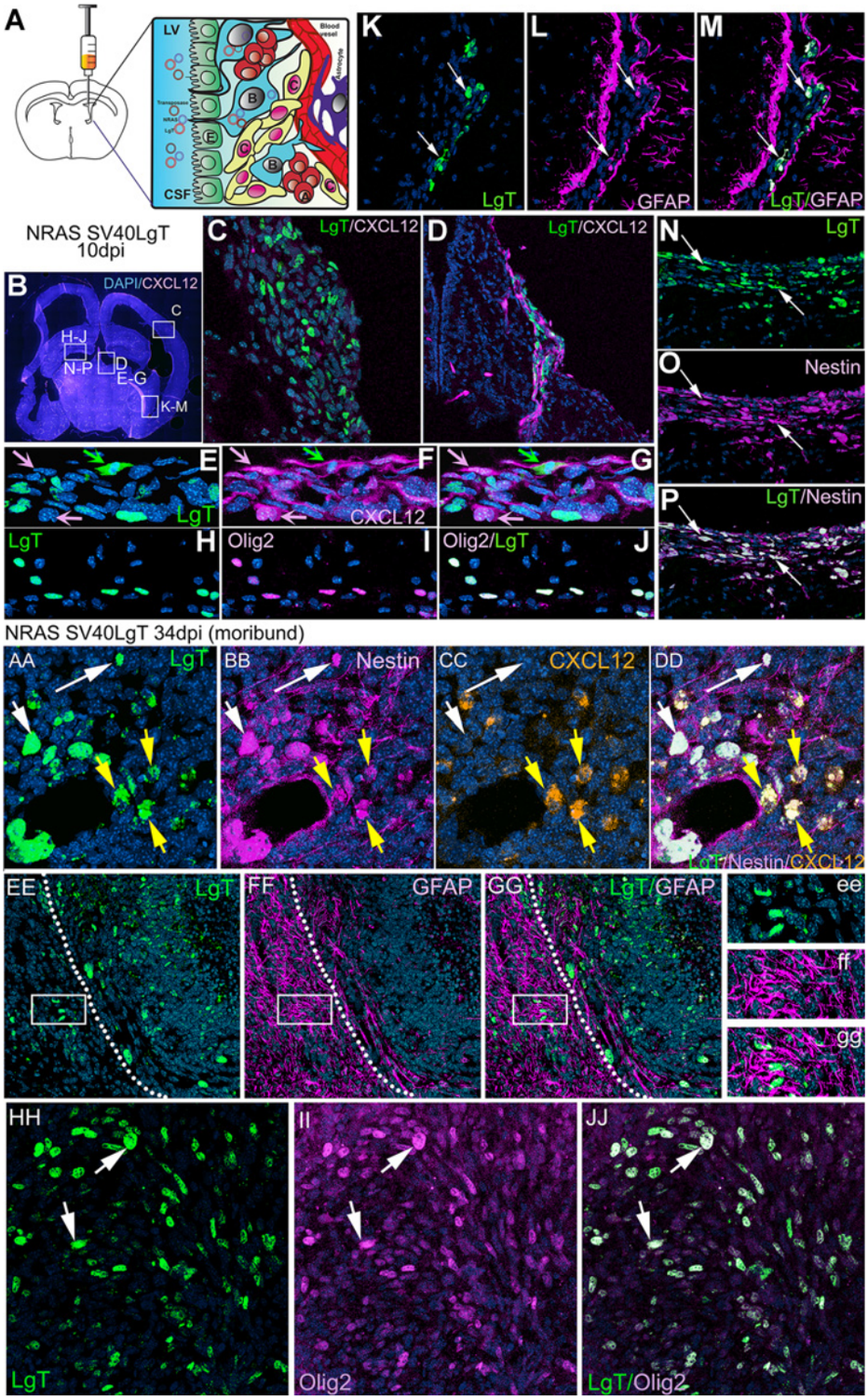

Figure 1.

Gliomas induced by transforming NPCs in neonatal mice with oncogenic DNA express markers characteristic of NSCs and GSLCs: Nestin, GFAP, and Olig2. **A**, Schematic representation of the method used to induce NSC-derived glioblastoma. Plasmids encoding the Sleeping Beauty transposase and oncogenic DNA, flanked by transposable elements, are injected into the lateral ventricle of postnatal day one mice. The DNA is taken up by neural stem cells (B cells), in direct contact with the lateral ventricle through their cilium, which protrudes in between the ependymal (E) cells lining the ventricle. Normally, B cells will give rise to transient amplifying cells (C cells) which then differentiate into migrating neuroblasts (A cells). (*Continued on the following page.*)

notably the ones in the proximity of endothelial cells express CXCL12 (Fig. 1E–G).

At 19 dpi, several larger tumors developed, some still in contact with the lateral ventricles (Supplementary Fig. S1B and S1G) and some within the brain parenchyma (Supplementary Fig. S1F and H). At this time, all transformed cells still express Nestin (Supplementary Fig. S1F) and Olig2 (Supplementary Fig. S1H), whereas only some of the cells within the tumor area express GFAP (Supplementary Fig. S1G). The most intense expression of GFAP is noted in the brain surrounding the tumor, an area of reactive astrogliosis (Supplementary Fig. S1G and Fig. 1EE–GG). In tumors from moribund animals, transformed cells continue to express Nestin (Fig. 1AA–DD), Olig2 (Fig. 1HH–JJ); some of the $Nestin^{+}$ and LgT^{+} cells also express CXCL12 (Fig. 1AA–DD). Notably, at this stage, tumor cells have lost GFAP expression (Fig. 1 EE–GG).

Mature tumors also harbor the histologic hallmarks of human glioblastoma: large multinucleated transformed cells (Supplementary Fig. S2A), atypical mitoses (Supplementary Fig. S2F), vascular proliferation (Supplementary Fig. S2B), pseudo-pallisading necrosis (Supplementary Fig. S2C), perivascular and diffuse invasion (Supplementary Fig. S2D and E), and hemorrhages (Supplementary Fig. S2E). These tumors are devoid of patent vascularization, as evidenced upon injection with fluorescent dextrans showing that blood vessels within the tumor lose the glia limitans (GFAP = magenta) and balloon into large cavities with leaky endothelia through which the dextrans diffuse into the surrounding tissue (Supplementary Fig. S2B).

Functional evidence of GSC identity is the ability to generate tumors upon intracranial transplantation which recapitulate the cellular heterogeneity present in the parental tumor (36).We have shown that Sleeping Beauty–derived cells self-renew in culture and grow as neurospheres in serum-free conditions (31, 37) and hereby demonstrate that newly generated neurospheres implanted orthotopically in mice generate aggressive tumors which recapitulate molecular and histologic features of the original tumor and render animals moribund in less than 30 days (Supplementary Fig. S3A). In addition, neurospheres generated from these tumors express on their surface the GSC marker, CD133 (prominin; Supplementary Fig. S3B), the first marker used to identify GSCs in human glioblastoma (38); widely employed to isolate GSCs from human glioblastoma.

Ependymal cells, the cells lining the lateral ventricles, equipped with motile cilia that contribute to the flow of CSF, are less likely to take up the injected plasmids as they do not proliferate postnatally (39). To test whether ependymal cells are transformed in the present model, we analyzed expression of Myosin-VIIa, an actin-binding molecular motor protein, in relation to GFP-expressing cells transduced with transposons encoding a short hairpin p53-GFP, PDGF, and NRAS(SPN) (34). We show that transformed tumor cells do not express Myosin-VIIa, and are thus unlikely to originate from ependymal cells, are immediately adjacent to them, and display radial glia morphology (Supplementary Fig. S3C). As we cannot distinguish whether these cells are NSCs (type B) or transient amplifying cells (type C), we conclude that in this model, tumors are induced through the transformation of NPCs and that transformed cells harbor molecular and functional characteristics of GSLCs.

The pleiotropic chemokine CXCL12 and its cognate receptor CXCR4 are expressed in multiple cell types within the tumor and normal brain

Accumulating data highlight the importance of secreted factors within the GSC niche in maintaining the identity and malignancy of GSLCs (40). To identify chemokines secreted by NPC-derived glioblastoma cells, we analyzed gene expression in M7 neurospheres, generated with NRAS and SV-40 LgT (34) and compared it with two other glioblastoma cell lines: GL26, generated from intracranial tumors chemically induced with methyl-cholantrene, propagated in animals and in culture for more than half a century (41) and a cell line derived from GL26 cells (GL26A1), modified to express shp53, NRAS, and PDGF (SPN), genetic modifications relevant for human glioblastoma. Details of this microarray experiment are described in the Supplementary Methods. This analysis yielded 5,866 probe sets differentially expressed between M7 and GL26, 5,270 between M7 and GL26A1, and 470 between GL26A1 and GL26 (Supplementary Table S1). Several chemokines showed highest expression in the M7 cells, notably CCL2, CXCL1, CCL7, and CXCL12 (Supplementary Fig. S4A). We validated these changes in expression with PCR and qPCR (Supplementary Fig. S4B and S4C). Increased expression of CXCL12 in

(*Continued.*) Uptake and transposon-mediated genomic integration of oncogenic DNA into NSC cells gives rise to transformation of proliferating C cells into tumor cells and their guided division and migration alongside blood vessels (**D**) or diffusely through the forebrain parenchyma (**C**) to generate tumors with glioblastoma characteristics. **B**, 10 dpi a coronal section through the brain of an 11-day-old mouse ($CXCL12^{dsRed}$) injected at P1 with NRAS and SV-40 LgT. White rectangles represent areas depicted in panels **C**, **D**, **E–G**, **H–J**, **K–M**, and **N–P**. **C**, Region of diffuse tumor cell proliferation ventral to the cortex and bordering the enlarged ventricle shows expression of LgT in transformed cells invading into the brain parenchyma. **D,** Region of tumor cell migration (green, LgT positive) alongside CXCL12-positive endothelial cells (magenta), close to the midline choroidal plexus in the lateral ventricle. Some cells are double positive for CXCL12 and LgT. **E–G,** Enlarged area from **D** illustrating colocalization of LgT (green) and CXCL12 (magenta) in some cells (green arrow), whereas most CXCL12-positive cells (vascular endothelial cells) do not express LgT (pink arrows). **H–J,** Region bordering the lateral ventricle where LgT-positive cells (green) are shown to express the glioma stem cell marker Olig2 (magenta). **K–M,** Region of the lateral ventricle at the ventral interface between the hippocampus and cortex where LgT-expressing tumor cells (green) are shown to coexpress GFAP (white arrows). Visible to the left and right of the transformed cells are the rows of $GFAP^{+}$ neural stem cells of the SVZ. **N–P**, Region of tumor cell proliferation ventral to the hippocampus illustrating colocalization of all LgT-positive cells (green) with the NSC marker nestin (magenta) (white arrows). Note the stream of tumor cells invading away from the ventricle into the brain parenchyma. The nuclear stain DAPI (blue) was used in all panels. **AA–DD,** Magnified view of a region within the core of the tumor showing LgT-positive cells (green) expressing Nestin (magenta) and some cells also express CXCL12 (orange). White arrows in **AA–DD** point to cells coexpressing LgT and Nestin, whereas yellow arrows point to cells expressing all three markers: LgT, Nestin, and CXCL12. **EE–GG** illustrate a region at the margin of the tumor (dotted white line) showing extensive staining with GFAP outside the tumor border (magenta), indicative of a massive reactive gliosis. LgT-positive cells (green) do not express GFAP, not even the invasive cells migrating outwards from the tumor (white rectangle in **E–G** and **ee–gg**). **HH–JJ,** Tumor cells from moribund animals (LgT+ green) continue to express the glioma stem cell marker Olig2 (magenta). All LgT+ cells are Olig 2 positive.

NPC-derived glioblastoma cells was of interest, as this chemokine has been shown to regulate neural and hematopoietic stem cell niches (16, 35).

We analyzed by qPCR expression of CXCL12 and of its cognate receptor CXCR4 in dissected tissue from either the tumor or normal brain of moribund tumor-bearing animals with newly generated tumors induced with either NRAS/LgT or SPN (Supplementary Fig. S4D). Data show that expression of *cxcl12* is higher in the tumor and brain from animals with NRAS/LgT-induced tumors, compared with SPN-induced tumors (Supplementary Fig. S4D). This could reflect the developmental decrease in expression of this cytokine (42), as NRAS/LgT-injected animals become moribund within their first month of life. We have previously shown that SPN-injected animals have a median survival (MS) of 62.5 days, twice as long as NRAS/LgT (MS = 30 days; ref. 31). Expression of *cxcl12*, on a per cell basis, is similar between the tumor and the brain; however, considering the high cellularity of the tumor area, we reason that overall, expression of *cxcl12* is higher in tumor-bearing animals. Expression of *cxcr4* is increased in the tumor compared with the normal brain (Supplementary Fig. S4D). IHC revealed high expression of CXCR4 within the numerous tumor-infiltrating mononuclear cells identified with CD45 (Supplementary Fig. S4E). qPCR analysis showed maximal expression of *cxcr4* in immune infiltrating myeloid cells ($CD45^+CD11b^+Gr1^+$; Supplementary Fig. S4F), indicating that the observed increase of *cxcr4* is likely due to the increase in immune infiltrating cells. Analysis of CXCR7, the other receptor which can bind CXCL12 (43), revealed expression 20- to 30-fold lower than CXCR4 in NPC-derived tumor cells (data not shown), reason for which we focused our further analyses solely on CXCR4.

Immunohistochemical analysis of CXCL12 and CXCR4 showed that both the chemokine and its receptor are ubiquitously expressed within the tumor and normal brain (Fig. 2). CXCL12 is expressed in multiple cells including neurons and astrocytes within the cortex and the hippocampus (Fig. 2B, b and C, c), in vascular endothelial cells in the normal brain and tumor (Fig. 2D and F). High expression of CXCL12 is found within areas in the center of the tumor, possibly areas of hypoxia (Fig. 2F and G), as well as in invading streams of tumor cells at the tumor border (Fig. 2D and E). CXCR4 expression is predominant in vascular endothelial cells within the normal brain and tumor (Fig. 2 BBbb, EEee) and also in regions of necrosis, highly infiltrated with immune cells (Fig. 2EEee, FFff, GGgg). Expression of CXCR4 is also found in neurons of the hippocampus and large multinucleated tumor cells, some of which come in contact with CXCR4-expressing monocytes (Fig. 2DDdd).

Taken together, these data illustrate the ubiquitous presence of both CXCL12 and CXCR4 within the tumor and the brain, expression congruent with the pleiotropic functions of this signaling axis, involved in development, chemotaxis, migration, proliferation and survival of neurons, glia, tumor, and hematopoietic cells (44, 45).

Treatment of NPC-derived glioblastoma neurospheres with the CXCR4 antagonist: AMD3100 induces apoptosis and decreased cell-cycle progression

It was reported that AMD3100 (plerixafor) inhibits proliferation and induces apoptosis of U87MG human glioblastoma cells *in vitro* and *in vivo* (25). Another study using U251 and also U87MG human glioblastoma cells demonstrated that AMD3100 by itself had no effect on the initial tumor progression; however, it improved survival of tumor-bearing animals by inhibiting the infiltration of $CD11b^+$ cells into the radiated tumor bed and prevented tumor recurrence, attributed to decreased vasculogenesis after irradiation (26).

To test whether AMD3100 modulates cell death in primary NPC-derived glioblastoma cells, we analyzed apoptosis in a N/LgT cell line (M7) over a time course of 5 days. Results show an increase in early apoptosis after 72 and 120 hours of treatment (Fig. 3A). Proliferation analysis in three different N/LgT (M1, M4, and M7) and shp53-NRAS-PDGF (OL61) neurosphere cultures demonstrate that blocking CXCR4 markedly inhibits their proliferation upon prolonged exposure to the drug (more than 72 hours; Fig. 3B). AMD3100 treatment showed a consistent decrease in proliferation in all neurosphere cultures tested, ranging between 34% and 59% of control after 96 hours of treatment and 23%–53% at 120 hours (Supplementary Table S2).

Cell-cycle analysis was performed on three different N/LgT neurosphere cultures and results show that AMD3100 significantly reduced the number of cells entering S-phase in all three neurosphere cultures tested (Fig. 3C), indicating that blocking CXCR4 inhibits cell-cycle progression retaining most of the cells in G_2–M.

The tumor suppressor retinoblastoma (Rb) pathway is altered in more than 70% of human glioblastomas (46). Decreased Rb function due to mutations, alterations in the Rb pathway, or due to the binding and inactivation of Rb by transforming proteins, like the SV40 LgT (47), leads to the release of inhibition of the E2F transcription factors and subsequent cell-cycle progression and predisposition to malignancies (48). We analyzed the expression of Rb and phosphorylated $Rb^{S807/811}$ in lysates from M1 and M7 cells treated or not with AMD3100 over a time course of 120 hours. We show that AMD3100 elicited a decrease in Rb and pRb after 72-hour and 120-hour time points (Fig. 4A), which correspond with increased apoptosis in the NPC-derived glioblastoma cells (Fig. 3A).

Akt is a serine/threonine signaling kinase downstream of RTKs, which signal through PI3K to promote cellular growth and survival. Large-scale genomic analyses of glioblastoma have shown increased activation of Akt, as evidenced by increased levels of phosphorylated Akt (pAkt) in the majority of glioblastoma samples and cells (49), this being attributed to both overactivation of multiple RTKs (EGRF, PDGFRA, FGFR1, VEGFR2) and also to the functional loss of the tumor suppressor PTEN, a strong negative regulator of Akt (50, 51). We analyzed the expression of $pAkt^{S476}$ in NPC-derived glioblastoma neurospheres, and hereby show that plerixafor decreased expression of $pAkt^{S476}$ (Fig. 4A).

CXCL12 promotes survival after injury of cortical neurons by regulating the ratio of pro- and antiapoptotic members of the Bcl-2 family of proteins (52). Also, resistance to TRAIL-induced apoptosis in glioblastoma has been linked to the increase in the antiapoptotic protein Bcl-XL (53). Expression analysis of Bcl-XL following treatment with plerixafor shows a decrease after 120 hours (Fig. 4A). These data suggest that plerixafor promotes apoptosis of glioblastoma cells through modulating the PI3K/PIP2, 3/Akt pathway, and also by inhibiting antiapoptotic molecules of the Bcl-2 family, like Bcl-XL.

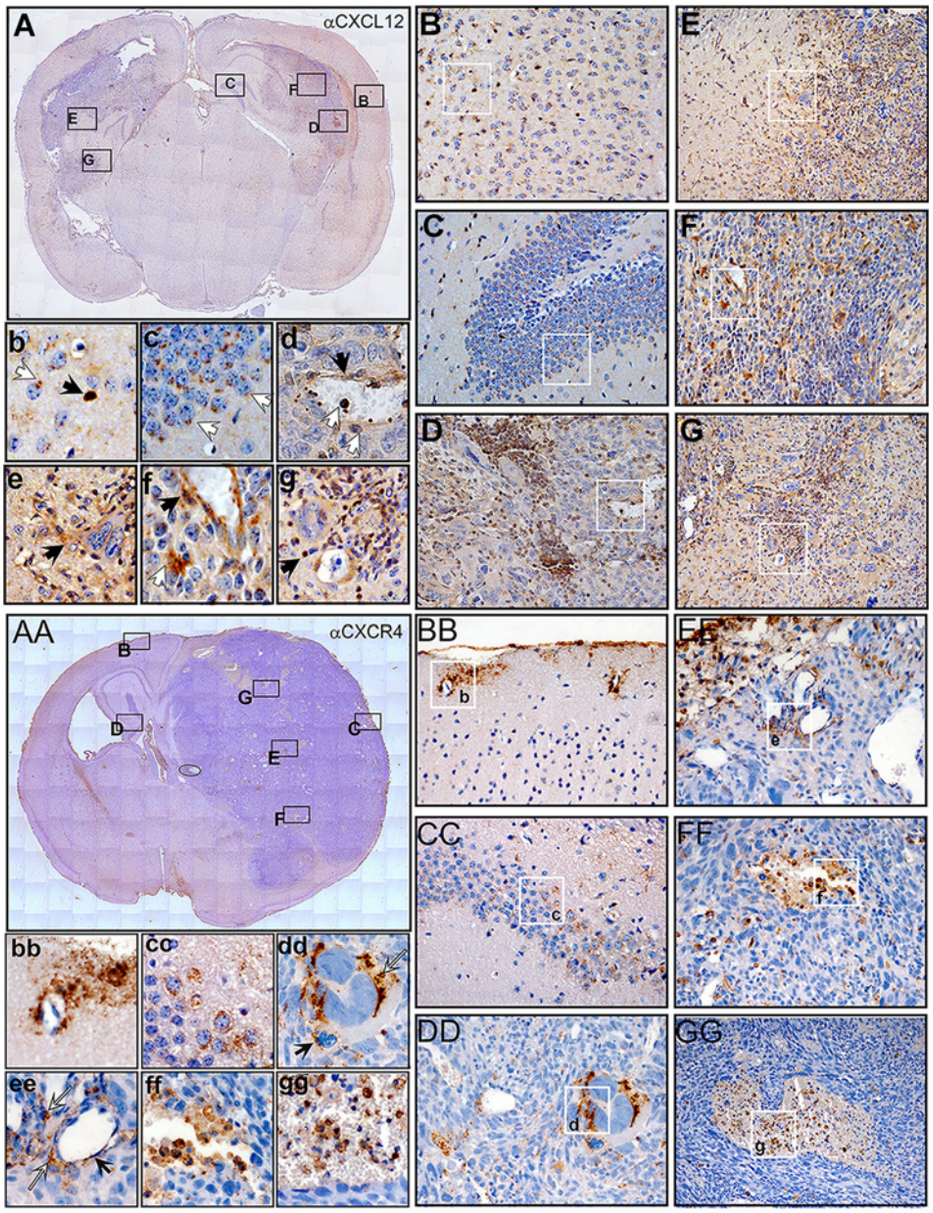

Figure 2.

CXCL12 and CXCR4 are expressed in multiple cell types within the tumor and normal brain. **A–G**, IHC for CXCL12. **A,** Coronal section through the brain of a mouse harboring a tumor induced with NRAS and SV40 LgT. Rectangles represent areas depicted in the larger panels: **B,** Cortical region; **C,** Hippocampus; **D** and **F,** Tumor core; **E** and **G,** Tumor margin. **B**/**b,** In the cortex neurons (white arrow in **b**) and glia (black arrow in **b**) express low and high levels of CXCL12 respectively. **C**/**c,** In the hippocampus, granule cells show polarized expression of CXCL12. **D**/**d,** Within the tumor, CXCL12 is present in endothelial cells black arrow in **d** and **f**, in infiltrating immune cells (white arrows in **d**), and in invasive streams of tumor cells (**D** and **E**/**e**). Regions within the tumor show cells with high expression of CXCL12 (**D, G**, white arrow in **f**, black arrow in **g**). **AA–GG,** IHC for CXCR4. **AA,** Coronal section through the brain of a moribund mouse harboring a tumor induced with NRAS and SV40LgT. Rectangles represent areas depicted in the larger panels: **BB,** Cortical region; **CC,** Hippocampus; **DD**, **FF**, and **GG,** Tumor core; and **EE**, The brain and tumor margin. **BB**/**bb,** In the cortex, expression of CXCR4 is mainly evident within and surrounding vascular walls. **CC**/**cc,** In the hippocampus, granule cells show low expression of CXCR4. **DD**/**dd,** Within the tumor CXCR4 is present in some tumor cells and in tumor-infiltrating mononuclear cells. White arrow (**dd**) points to a large multinucleated tumor cell expressing CXCR4 and black arrow (**dd**) points to a CXCR4-expressing monocyte/macrophage. **EE**/**ee,** At the edge of the tumor and brain enlarged vessels show expression of CXCR4 within the endothelia (black arrow in **ee**) and also in tumor-infiltrating immune cells (white arrows in **ee**). **FF**/**ff** and **GG**/**gg,** Within the tumor core enlarged vessels turn into necrotic regions in which numerous immune infiltrating cells are expressing high levels of CXCR4.

Expression of Cyclin D1 and of its binding partners *cdk4* and *cdk6* were analyzed by Western blot analysis and qPCR. Results demonstrate that plerixafor inhibits transcription of cyclin D1, *cdk4* and *cdk6* (Fig. 4B), critical for cell-cycle progression in early G_1, but has no effect on the expression of cyclin E or p21 (data not shown).

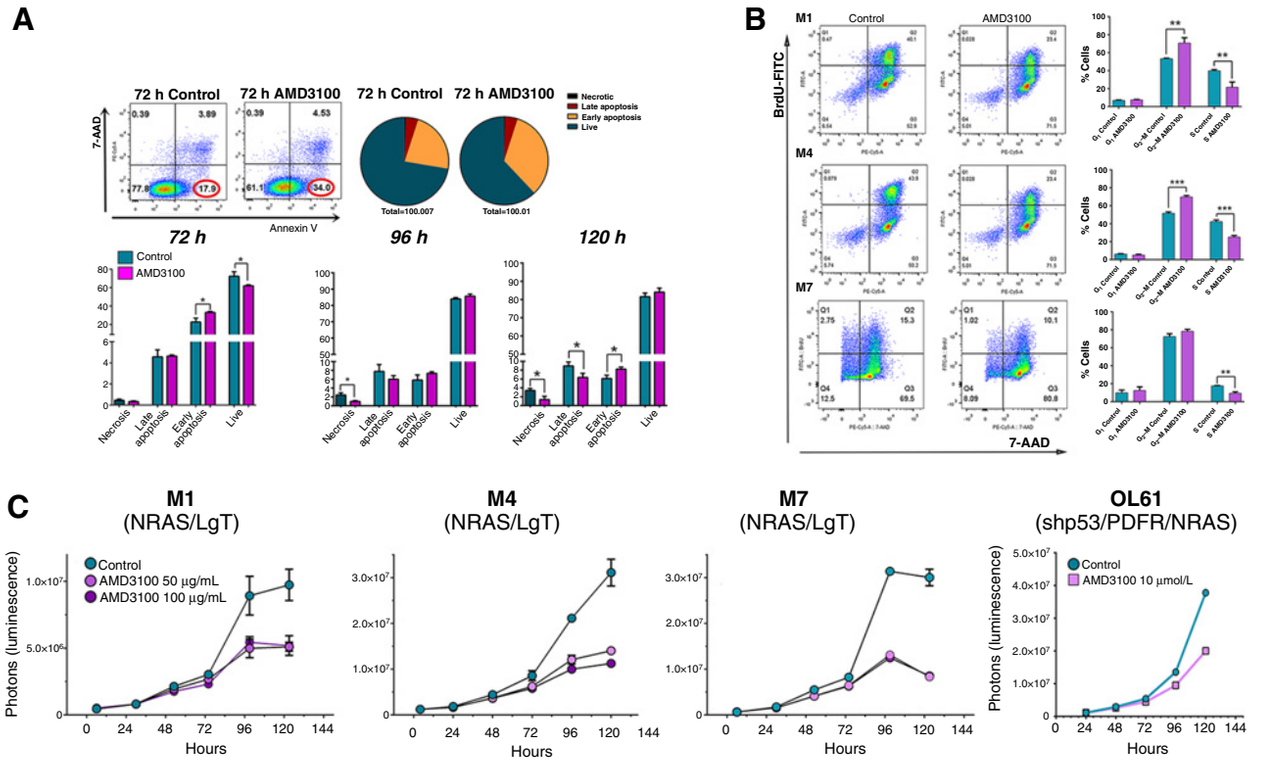

Figure 3.

Treatment of NPC-derived GSCs with AMD3100 (plerixafor) induces apoptosis, decrease in cell proliferation, and arrests cells in the G_2–M phase of the cell cycle. **A,** Representative dot plots of M7 (NRAS/LgT) cells treated or not with AMD3100 for 72 hours and stained with Annexin V- FITC (horizontal axis) and the fluorescent DNA dye 7-amino-actinomycin D (7-AAD, vertical axis). Pie charts represent the quantitative distribution of cells within each treatment group: live cells (Annexin V negative and 7AAD negative, hunter-green), early apoptotic cells (Annexin V positive, 7-AAD negative, orange), late apoptosis (Annexin V positive, 7-AAD positive, red), necrotic (Annexin V negative, 7-AAD positive, black). Bottom, quantitative analysis of the distribution of live, necrotic, and apoptotic cells during the 5-day treatment with AMD3100. **B,** Proliferation analysis of four different glioblastoma cell lines induced with NRAS and LgT (M1, M4, M7) or shp53/PDGF/NRAS (OL61) during a time course of 120 hours treated or not with AMD3100. **C,** Cell-cycle analysis of M1, M4, and M7 after 96 hours of treatment with AMD3100 and a one-hour pulse of BrdUrd. Cells were stained for BrdUrd-FITC and 7-AAD and analyzed by flow cytometry. Representative dot plots are presented to the left and quantitative analysis of cell-cycle phase distribution is presented to the right (G_1, BrdUrd negative, 7-AAD low; G_2–M, BrdUrd negative, 7-AAD high; and S-phase, BrdUrd positive; unpaired, two-tailed *t* test; *, $P < 0.05$; **, $P < 0.01$; ***, $P < 0.001$).

CXCL12/CXCR4 signaling operates in NPC-derived glioblastoma cells under hypoxic stress via an autocrine-positive feedback loop

CXCL12 is induced by hypoxia following irradiation (17, 26) and this is thought to be caused by TGFβ derived from glioma cells (54). As we observed an antiproliferative effect of AMD3100 only after prolonged exposure to the inhibitor, we analyzed changes in the expression of *cxcl-12*, *cxcr-4*, *hif1-α*, and *tgf-β* within these cells during the 5-day time course. Results show that at 96 hours there is an approximately 6-fold increase of *cxcl-12*, which correlates with an increase in *hif1-α* and *tgf-β* (Fig. 4B). Expression of *cxcr4* does not change (data not shown). The increase in *tgf-β* and *cxcl12* is completely abrogated by the treatment with AMD3100, which had no effect on *hif1-α* mRNA. Furthermore, addition of exogenous CXCL12 partially rescued the decrease in proliferation induced by AMD3100, while it had no additive effect on proliferation in the absence of AMD3100 (Fig. 4C). These data suggest that the CXCL12/CXCR4 signaling pathway operates in NPC-derived GSLCs via an autocrine feedback loop, regulating their survival and proliferation.

Neurosphere cultures derived from N/LgT tumors show similar molecular characteristics with human glioma cells

Infection with SV-40 is not considered to cause development of glioblastoma; there are, however, reports showing expression of SV40 T antigen in glioblastoma patients (55, 56). Nonetheless, the transforming actions of LgT result in many molecular changes encountered in human glioblastoma. Also, activations of RTK/RAS/PI3K pathways are very commonly (88%) observed in human glioblastoma (46). Activation of Ras has been used in preclinical models of glioblastoma (37, 57–59) demonstrating that it represents a suitable genetic driver for induction of mouse glioblastoma, which recapitulate the salient features of human disease. We hereby show that mouse glioblastoma neurospheres induced with N/LgT exhibit similar molecular characteristics with human glioblastoma cells.

Expression of several molecular players, known to be important in human glioblastoma was compared in N/LgT-derived neurospheres and in the human glioblastoma cell lines: U251 and U87, commonly used in preclinical models of glioblastoma and HF2303, a primary GSLC line derived from a

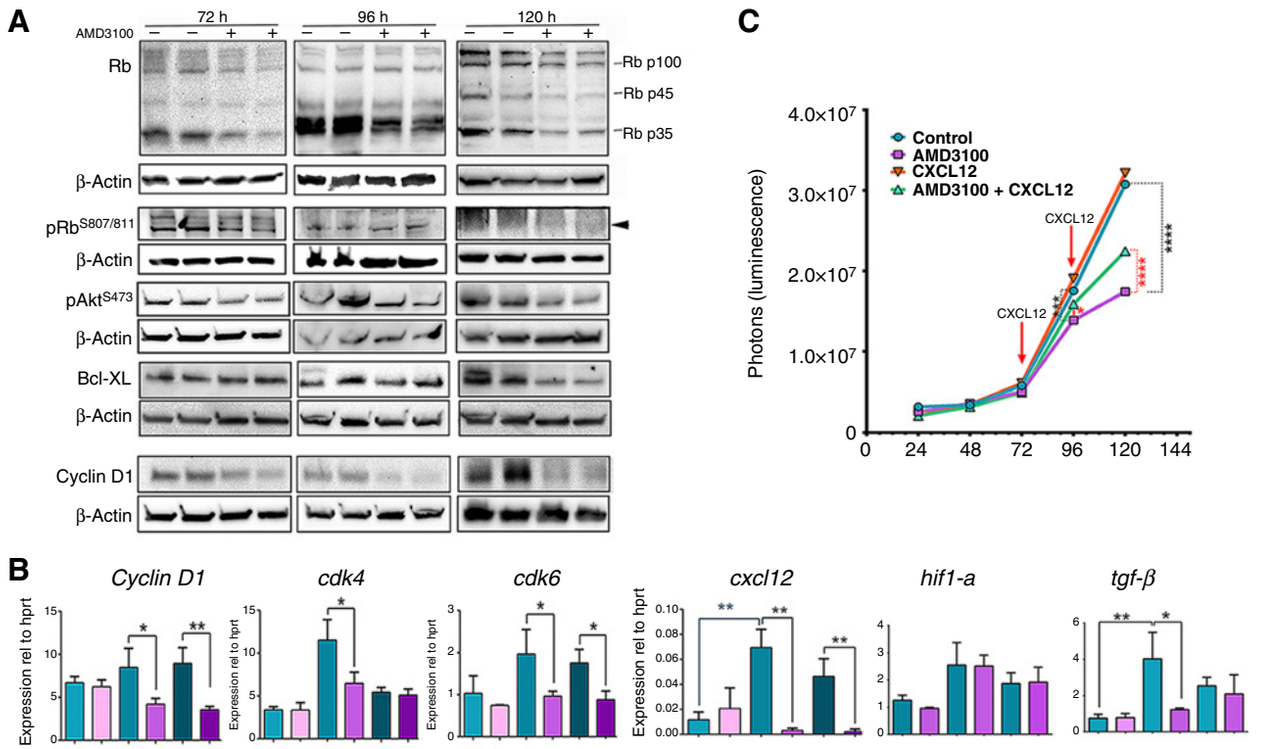

Figure 4.

Treatment of NRAS/LgT derived glioblastoma cells with AMD3100 (plerixafor). **A,** Western blot analysis of M7 (NRAS/LgT) cells probing with antibodies against retinoblastoma (Rb and phospho-Rb$^{S807/811}$), pAkt, Bcl-XL, and Cyclin D1 during a 5-day time-course of AMD3100 treatment. Lanes represent duplicate treatment flasks with (+) or without (-) AMD3100. β-Actin was used as a loading control. **B,** qPCR analysis of gene expression in cells treated or not with AMD3100, during a 5-day time course, to analyze the expression of *cyclin D1, cdk4* and *cdk6*, cxcl12, hif1-α, and tgf-β represented graphically as relative expression compared with *hprt*. Error bars, SEM of triplicate treatment wells. **C,** Cell proliferation analysis of M7 (NRAS/LgT) cells treated or not with AMD3100 (10 μmol/L) and CXCL12 (20 nmol/L) showing that exogenous CXCL12 rescues the AMD3100 decrease in proliferation, but does not increase proliferation in the absence of AMD3100 statistical test: two-way ANOVA with Bonferroni correction for multiple comparisons. (*, $P < 0.05$; **, $P < 0.01$; ***, $P < 0.001$; ****, $P < 0.0001$).

gliosarcoma patient (60). pAkt^{S476} is elevated in N/LgT neurospheres when compared with primary mixed glia cells (MG) isolated from the brain of a 3-day-old mice (Fig. 5A, left). Similarly, pAkt^{S476} is increased in human glioma cells over normal human astrocytes (NHA; Fig. 5A, right). GFAP expression is low in N/LgT-derived neurospheres as well as in human glioma cells grown in serum-free conditions. Expression of PTEN is absent in U251 glioma cells and reduced in U87, and also decreased in N/LgT-derived cells, whereas expression of the pERK1/2 is more variable when compared with MG and NHA, respectively (Fig. 5A).

Treatment with AMD3100 reduces the expression of HIF1α in NPC-derived glioma neurospheres and human glioma cells

We analyzed the three human cell lines for their proliferation in the presence of AMD3100 and for their expression of CXCL12 and CXCR4. Results show that, AMD3100 decreased proliferation of the human U251 (Fig. 5B) and HF2303 GSCL cells (Fig. 5C) grown in serum-free media, after long-term exposure to the inhibitor, albeit to a much lesser degree than the mouse NPC-derived neurospheres, and that it had no effect on the growth of U87 cells (data not shown). Both U251 and HF2303 cells express CXCL12 and CXCR4, whereas U87MG cells express CXCR4, but not CXCL12 (qPCR data, not shown).

We had shown that after 96 hours in culture *hif-1a* mRNA (Fig. 4B) is increased in M7 cells which grow robustly and form large neurospheres. In contrast, U251 and HF2303 cultured in serum-free conditions grow slower, as a mixture of small neurospheres and adherent cells. To test whether plerixafor changes the expression of survival and cell-cycle progression signaling molecules in human glioblastoma cells, as we have shown for mouse NPC-derived glioblastoma cells (Fig. 4A), we employed a method to induce hypoxic stress with cobalt chloride ($CoCl_2$) in both mouse (M7) and human glioblastoma cells cultured in serum-free conditions. We show that incubation with $CoCl_2$ induces the expression of HIF-1α in both mouse and human cells and this induction is strongly inhibited by the addition of plerixafor in M7, U251, and also in HF2303 (Fig. 5D). Similar to the long-term time-course analysis in M7 cells, plerixafor also inhibits pAkt, pRb, Rb, Cyclin D1, and Bcl-XL in M7 cells, and to a lesser degree in U251 cells (Fig. 5D).

Animals bearing *de novo* glioblastomas induced from NPCs treated with AMD31000 survive longer

To test whether treatment with plerixafor is beneficial for tumor-bearing animals we induced tumors with N/LgT in P1 day mice and monitored tumor formation with bioluminescence. At 21–24 dpi, when macroscopic tumors developed, animals were

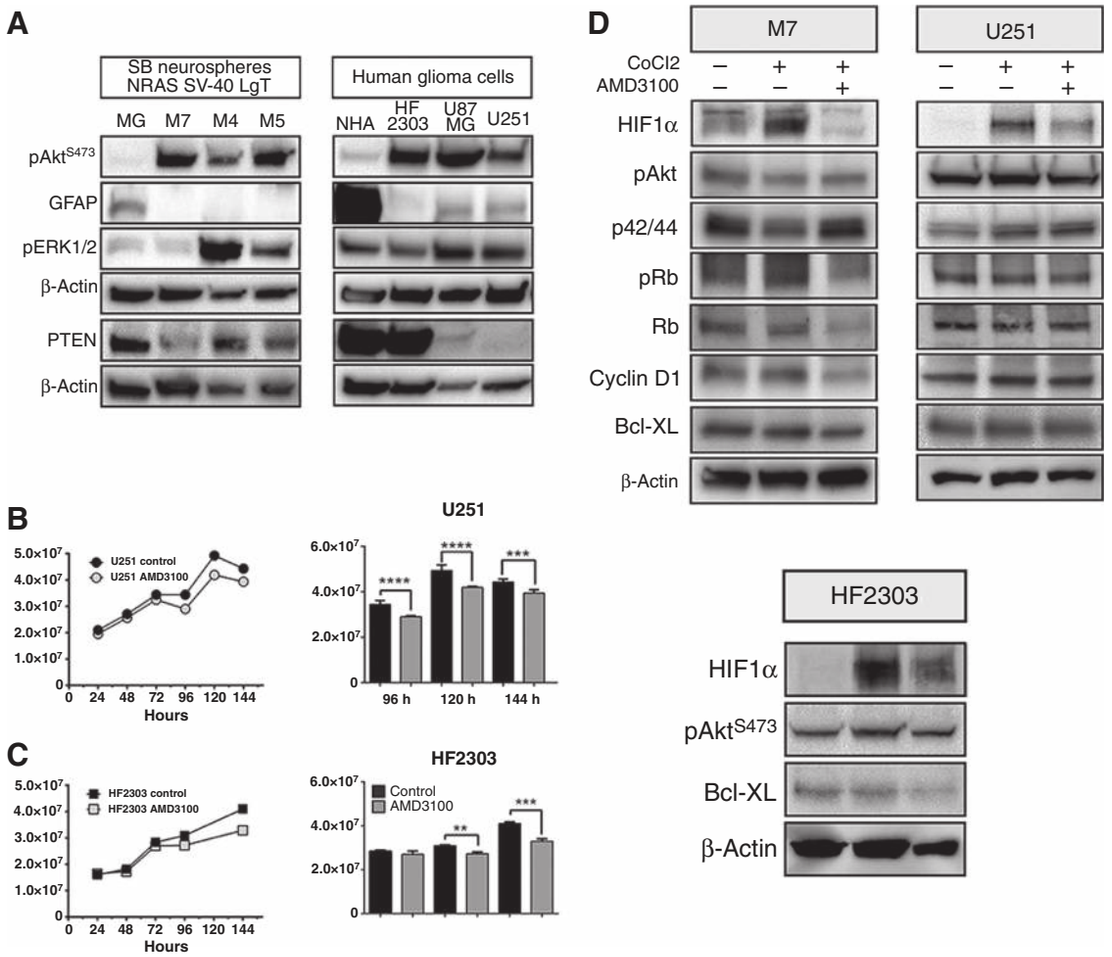

Figure 5.

A, Neurosphere cultures derived from NRAS/LgT tumors show similar molecular characteristics with human glioma cell lines. Left, a Western Blot analysis showing expression of pAkt^{S473}, GFAP, pERK1/2, PTEN, and β-actin in NRAS/LgT NPC-derived glioblastoma neurospheres (M7, M4, M5) and mixed glia (MG) isolated from the brain of postnatal day 3 mice. Right, represents a Western blot analysis of the same proteins in human glioblastoma cells (HF2303, U87MG and U251 compared with normal human astrocytes (NHA). **B** and **C,** AMD3100 decreases proliferation of human glioblastoma cells after long-term culture in NSC media. Growth curves of U251 (**B**) and HF2303 (**C**) human glioma cells and bar graph comparisons in control and AMD3100 (10 μmol/L) treated cells over a 6-day (144 hours) time course. Significant differences as analyzed by two-way ANOVA with Bonferroni correction for multiple comparisons are represented by asterisks (**, $P < 0.01$; ***, $P < 0.001$; ****, $P < 0.0001$) **D**, Top, treatment with AMD3100 reduces the expression of HIF-1α in M7 neurospheres and human glioma cells U251. Western blot analysis of M7 and U251 glioblastoma cells after treated or not with $CoCl_2$ and AMD3100 for 2 hours showing expression of pAkt, p42/44, pRb, Rb, CyclinD1, Bcl-XL, and β-actin. Bottom, treatment with AMD3100 reduces the expression of Hlf-1α, pAKT, and Bcl-XL in human HF2303 cells.

implanted with osmotic pumps containing either saline or AMD3100 (15 mg/kg/day). Animals were sacrificed after 5 days of treatment. Six hours prior to sacrifice, animals were pulsed with bromodeoxyuridine (BrdUrd) to analyze *in vivo* cell-cycle progression. Data show a decrease in BrdUrd uptake by tumor cells after 5 days of AMD3100 treatment. Analysis of tumor area, at the site of maximum tumor diameter, showed a decrease in size, which however did not reach statistical significance, due likely to the variability of the tumors when using this model (Fig. 6A). Tumors in animals treated with AMD3100 showed a decrease in spread, being mainly confined to one hemisphere (Supplementary Fig. S5), indicating a possible role of CXCL12 in promoting invasion of these glioblastoma cells. The MS of animals treated with AMD3100 osmotic pumps (53 days) was significantly increased ($P < 0.0001$, log-rank test) when compared with non-treated animals (30 days), indicating a slower progression of the disease with CXCR4 blockade (Fig. 6B).

To ascertain that the phenotype observed is due to the signaling through CXCR4, we have also phenocopied the *in vitro* and *in vivo* effects seen with AMD3100 treatment by two genetic means. First, we used the Cre/LoxP system, crossing mice expressing Cre recombinase under the control of the Nestin promoter, with mice which have the exon2 of the *CXCR4* gene flanked by loxP sites. We injected neonatal animals from the Nestin-Cre/CXCR4$^{loxP/loxP}$ × CXCR4$^{loxP/loxP}$ crosses with N/LgT, monitored tumor formation, and sacrificed the animals at the first signs of tumor burden. Tumors were dissected, neurospheres generated, and grown in serum-free media to expand. qPCR analysis shows that

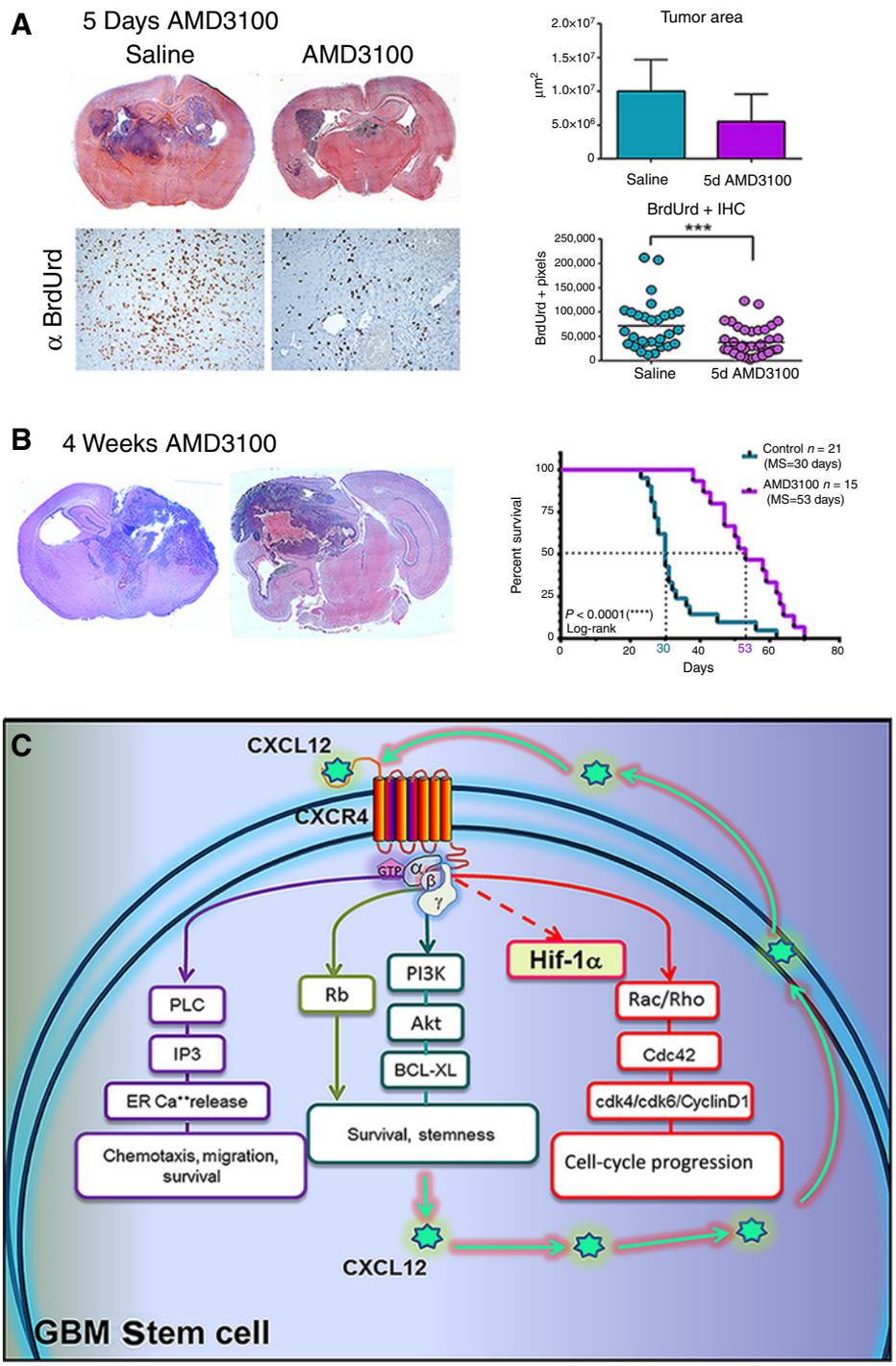

Figure 6.

A, Treatment of tumor-bearing mice with AMD3100 increases their survival and decreases cell-cycle progression of tumor cells. Top, hematoxylin and eosin–stained coronal brain sections from animals treated for 5 days with saline or AMD3100 and quantitation of tumor areas (S7) at their largest diameter ($n = 4$ per group). Bottom, representative micrographs of IHC detecting BrdUrd and quantitation of BrdUrd uptake in the tumors from animals treated with saline or AMD3100 (10 images per animal taken at 20× magnification). Unpaired, two-tailed t test was performed with GraphPad Prism (***, $P < 0.001$). **B,** Treatment with AMD3100 increases survival of animals bearing tumors induced with NRAS and SV40LgT. Left, representative coronal sections stained with hematoxylin and eosin from brains of moribund animals treated or not with AMD3100. Right, the survival curve comparing the median survival (MS = 53 days) of 15 animals treated with AMD3100 osmotic pumps with the survival of 63 untreated controls (MS = 30 days). Median survival was compared using the log-rank (Mantel–Cox) test showing significant difference (****, $P < 0.0001$). **C,** Schematic representation of the proposed mechanism of action of the CXCL12/CXCR4 signaling axis. CXCL12 produced by the tumor cells acts upon the GPCR receptor CXCR4 to activate multiple pathways. Activation of PI3K leads to the increase in pAkt and BCL-XL promoting survival and stemness. Activation of the Phospholipase C also leads to release of calcium from intracellular stores and triggers chemotaxis and migration and promotes survival. Activation of the Rho family of GTPases Rac/Rho and Cdc42 leads to microtubule reorganization, increased transcription and translation of Cyclin D1, CDK4 and CDK6 and to cell-cycle progression. Under hypoxic conditions, CXCL12 may induce the expression of HIF-1α.

Cre-expressing cells have lost expression of CXCR4 (Supplementary Fig. S6Aa) and cell proliferation analysis demonstrates that these cells have a decreased growth rate and that the response to AMD3100 is abrogated (Supplementary Fig. S6Ab and S6Ac).

Second, to determine the effect of CXCR4 knockdown on tumors generated with the Sleeping Beauty model shp53, NRAS, and PDGF, we used a lentiviral-mediated transduction of two short hairpin RNAs targeted against CXCR4 (sh1 and sh2) and a scramble, nontarget (NT) shRNA to modify the OL61 cells. qPCR and Western blot analysis show a reduction of 50% in the expression of CXCR4 in these cells (Supplementary Fig. S6Ba–S6Bc) and analysis of cell proliferation indicates a lower rate of proliferation and a decreased response to AMD3100 treatment when compared with the NT- shRNA transfected cells (OL61-NT;

Supplementary Fig. S6Bd and S6Be). Furthermore, when orthotopically implanted into C57BL6/J mice, OL61-sh2 cells generated tumors, significantly smaller in size when compared with OL61-NT at 10–11 dpi, and animals bearing OL61-sh2 tumors exhibited longer survival than the ones implanted with OL61-NT (Supplementary Fig. S6C).

Discussion

In this study, we identified CXCL12 to have highest expression in the most aggressive tumors induced using the Sleeping Beauty model generated with NRAS and SV40 LgT (31). We show that CXCL12 regulates the survival and proliferation of NPC-derived GSLCs through an autocrine-positive feedback loop initiated by hypoxic stimuli which also leads to enhanced expression of TGFβ, a potent immune suppressor. Treatment with plerixafor reduces both TGFβ and CXCL12. TGFβ has been proposed to induce expression of CXCL12, upstream of Hif-1α when controlling migration of hematopoietic stem and progenitor cells towards glioma cells (17). In the GSLC model presented herein, long-term treatment with plerixafor reduces both expression of CXCL12 and TGFβ, suggesting that the crosstalk between TGFβ and CXCL12 may be more complex and that inhibition of CXCL12 also downregulates TGFβ. Cyclin D1, cdk4 and cdk6 showed a similar pattern of expression with CXCL12 and TGFβ during the time course of plerixafor treatment linking these cell-cycle–regulating molecules to the autocrine signaling pathways downstream of CXCL12. Similarly, in malignant peripheral nerve sheath tumors, CXCL12 has been demonstrated to regulate expression of *cyclin D1* and *cdk4* and to a lesser extent of *cdk6,* and it has been shown that knockdown of CXCR4 prevents transition into S-phase arresting most cells (∼60%) in the G_0–G_1 phase of the cell cycle (61). Interestingly, treating GSCs with plerixafor also inhibits their progression into S-phase; however, most cells (60%–70%) are retained in G_2–M (Fig. 3C), suggesting an effect on microtubule dynamics during mitosis. In a model of treatment-resistant pancreatic cancer, in which the last avenue of chemotherapy is represented by docetaxel, an agent which binds microtubules and causes G_2–M mitotic arrest with subsequent induction of apoptosis, it has been shown that CXCL12 induces resistance to DTX by counteracting the DTX-induced microtubule stabilization (62). The arrest in G_2–M of GSCs cells following treatment with plerixafor suggests that in these cells, blocking CXCR4, in addition to the effect on the transcription and translation of cell-cycle–regulating proteins, also inhibits cell-cycle progression by stabilizing microtubules during mitosis. Paclitaxel, another member of the taxol family of microtubule-stabilizing chemotherapeutic agents is currently being tested for the treatment of glioblastoma in nanoparticle formulations with promising results (63). Combinatorial therapeutic approaches for glioblastoma with taxol compounds and CXCR4 inhibitors may improve the efficacy of the drugs and prevent resistance to treatment by counteracting the deleterious effect of CXCL12 on microtubule reorganization.

The current study also provides evidence that blocking CXCR4 induces apoptosis of NPC-derived glioblastoma neurospheres and this correlates with a decrease in pAkt, Rb, and Bcl-XL. The decrease in Rb was surprising as it was accompanied with a decreased cell-cycle progression, usually associated with increased Rb. An important tumor-suppressive function of Rb is thought to be maintaining the quiescence in stem cells, which is necessary for tissue homeostasis (64). In our study, in glioblastoma cells under hypoxic conditions treated with plerixafor, we observe a decrease in proliferation and a downregulation of the cell-cycle–regulatory proteins Cyclin D1, cdk4 and cdk6, accompanied by a decrease in Rb and pRb. One possibility is represented by a role of Rb in the survival of NPC-derived glioblastoma neurospheres under hypoxic stress, similar to its role in promoting neuronal survival under toxic stress (65). Given that loss of Rb function is present in human glioblastoma, hindering the ability of some pharmacologic cell-cycle inhibitors to inhibit proliferation (66), the availability of drugs which can inhibit the cell-cycle progression independent of Rb would be a useful addition to the antiglioma therapeutic toolbox.

In addition, we demonstrate that treatment with plerixafor inhibits the hypoxic induction of HIF1-α in mouse and human glioblastoma cells. It is known that hypoxia plays a pivotal role in the pathogenesis of cancers inducing angiogenesis, genomic instability, metabolic shift, survival, migration, and metastasis, these effects being mainly controlled by the increase of HIF-1α (30). Hypoxic conditions maintain GSCs and promote the cancer stem cell phenotype (67). Our data, showing inhibition of HIF1-α when blocking CXCR4 supports the existence of an autocrine CXCL12/CXCR4 signaling pathway within glioblastoma cells regulating their response to hypoxic stress, bringing new mechanistic insights on the importance of this signaling axis in glioblastoma pathogenesis.

Treatment of glioblastoma-bearing animals with AMD3100 alone did not yield long-term survivors in this very aggressive tumor model, which recapitulates many of the salient features of the human glioblastoma, including heterogeneity of tumors with respect to their size and location, regions of hemorrhage and necrosis, as well as vascular proliferation with the formation of glomeruloid blood vessels with poor blood perfusion. In this model, we show that, as the tumors increase in size, blood vessels entering the tumor balloon into large cavities with leaky endothelia (Supplementary Fig. S2B).The interior of the tumor remains poorly perfused. Thus, tumor cells located in these regions may not be exposed to the drug. Also, as these tumors are highly invasive (Supplementary Fig. S2A); tumor cells migrate and escape the hypoxic environment. These limitations related to drug bioavailability and characteristics of the tumor microenvironment, in which the drug is effective, need to be considered when testing agents for the treatment of glioblastoma. Our study brings new mechanistic insight and encourages further exploration of the use of drugs blocking CXCL12 signaling as adjuvant agents to target hypoxia-induced glioblastoma progression, prevent resistance to treatment, and recurrence of the disease.

Disclosure of Potential Conflicts of Interest

No potential conflicts of interest were disclosed.

Authors' Contributions

Conception and design: A.A. Calinescu, V. Yadav, P. Kadiyala, M.G. Castro
Development of methodology: A.A. Calinescu, V. Yadav, P. Kadiyala, D. Zamler, M.G. Castro
Acquisition of data (provided animals, acquired and managed patients, provided facilities, etc.): A.A. Calinescu, D. Tran, D. Zamler, R. Doherty, M. Srikanth, M.G. Castro
Analysis and interpretation of data (e.g., statistical analysis, biostatistics, computational analysis): A.A. Calinescu, V. Yadav, E. Carballo, P. Kadiyala, D. Tran, M. Srikanth, P.R. Lowenstein, M.G. Castro

Writing, review, and/or revision of the manuscript: A.A. Calinescu, V. Yadav, E. Carballo, P. Kadiyala, D. Zamler, P.R. Lowenstein, M.G. Castro
Administrative, technical, or material support (i.e., reporting or organizing data, constructing databases): A.A. Calinescu, P. Kadiyala, D. Tran, D. Zamler, R. Doherty, P.R. Lowenstein
Study supervision: A.A. Calinescu, P. Kadiyala, D. Zamler, P.R. Lowenstein, M.G. Castro

Acknowledgments

We gratefully acknowledge Mr. Philip Jenkins and the Department of Neurosurgery at the University of Michigan Medical School for their support of our work. We are also grateful to Dr. Karin Muraszko for her academic leadership, S. Napolitan, and M. Dahlgren for superb administrative support and M. Dzaman for outstanding technical support.

Grant Support

This work was supported by NIH/National Institute of Neurological Disorders & Stroke (NIH/NINDS) grants R37-NS094804, R01-NS074387, R01-NS057711, R21-NS091555, and R01-NS094804 (to M.G. Castro); NIH/NINDS grants R01-NS061107, R01-NS076991, R01-NS082311, and R21-NS084275 (to P.R. Lowenstein); Leah's Happy Hearts, University of Michigan Comprehensive Cancer Center, Chad Tough Foundation, and The Phase One Foundation (to M.G. Castro and P.R. Lowenstein); the Department of Neurosurgery, University of Michigan School of Medicine; the Michigan Institute for Clinical and Health Research, NIH 2UL1-TR000433; University of Michigan Cancer Biology Training Grant, NIH/NCI (National Cancer Institute) T32-CA009676; University of Michigan Training in Clinical and Basic Neuroscience, NIH/NINDS T32-NS007222; and the University of Michigan Medical Scientist Training Program, NIH/NIGMS (National Institute of General Medicine Sciences) T32-GM007863.

The costs of publication of this article were defrayed in part by the payment of page charges. This article must therefore be hereby marked *advertisement* in accordance with 18 U.S.C. Section 1734 solely to indicate this fact.

Received December 3, 2015; revised July 15, 2016; accepted August 1, 2016; published OnlineFirst August 19, 2016.

References

1. Ahmed AU, Auffinger B, Lesniak MS. Understanding glioma stem cells: rationale, clinical relevance and therapeutic strategies. Expert Rev Neurother 2013;13:545–55.
2. Zong H, Parada LF, Baker SJ. Cell of origin for malignant gliomas and its implication in therapeutic development. Cold Spring Harb Perspect Biol 2015;7:1–12.
3. Bao S, Wu Q, McLendon RE, Hao Y, Shi Q, Hjelmeland AB, et al. Glioma stem cells promote radioresistance by preferential activation of the DNA damage response. Nature 2006;444:756–60.
4. Bao S, Wu Q, Sathornsumetee S, Hao Y, Li Z, Hjelmeland AB, et al. Stem cell-like glioma cells promote tumor angiogenesis through vascular endothelial growth factor. Cancer Res 2006;66:7843–8.
5. Wang R, Chadalavada K, Wilshire J, Kowalik U, Hovinga KE, Geber A, et al. Glioblastoma stem-like cells give rise to tumour endothelium. Nature 2010;468:829–33.
6. Stiles CD, Rowitch DH. Glioma stem cells: a midterm exam. Neuron 2008;58:832–46.
7. Sanai N, Alvarez-Buylla A, Berger MS. Neural stem cells and the origin of gliomas. N Engl J Med 2005;353:811–22.
8. Caporaso GL, Lim DA, Alvarez-Buylla A, Chao MV. Telomerase activity in the subventricular zone of adult mice. Mol Cell Neurosci 2003;23:693–702.
9. Marian CO, Cho SK, McEllin BM, Maher EA, Hatanpaa KJ, Madden CJ, et al. The telomerase antagonist, imetelstat, efficiently targets glioblastoma tumor-initiating cells leading to decreased proliferation and tumor growth. Clin Cancer Res 2010;16:154–63.
10. Singh SK, Clarke ID, Terasaki M, Bonn VE, Hawkins C, Squire J, et al. Identification of a cancer stem cell in human brain tumors. Cancer Res 2003;63:5821–8.
11. Ligon KL, Huillard E, Mehta S, Kesari S, Liu H, Alberta JA, et al. Olig2-regulated lineage-restricted pathway controls replication competence in neural stem cells and malignant glioma. Neuron 2007;53:503–17.
12. Doetsch F, Caille I, Lim DA, Garcia-Verdugo JM, Alvarez-Buylla A. Subventricular zone astrocytes are neural stem cells in the adult mammalian brain. Cell 1999;97:703–16.
13. Mirzadeh Z, Merkle FT, Soriano-Navarro M, Garcia-Verdugo JM, Alvarez-Buylla A. Neural stem cells confer unique pinwheel architecture to the ventricular surface in neurogenic regions of the adult brain. Cell Stem Cell 2008;3:265–78.
14. Fuentealba LC, Obernier K, Alvarez-Buylla A. Adult neural stem cells bridge their niche. Cell Stem Cell 2012;10:698–708.
15. Calabrese C, Poppleton H, Kocak M, Hogg TL, Fuller C, Hamner B, et al. A perivascular niche for brain tumor stem cells. Cancer Cell 2007;11:69–82.
16. Goffart N, Kroonen J, Di Valentin E, Dedobbeleer M, Denne A, Martinive P, et al. Adult mouse subventricular zones stimulate glioblastoma stem cells specific invasion through CXCL12/CXCR4 signaling. Neuro Oncol 2015;17:81–94.
17. Tabatabai G, Frank B, Mohle R, Weller M, Wick W. Irradiation and hypoxia promote homing of haematopoietic progenitor cells towards gliomas by TGF-beta-dependent HIF-1alpha-mediated induction of CXCL12. Brain 2006;129:2426–35.
18. Komatani H, Sugita Y, Arakawa F, Ohshima K, Shigemori M. Expression of CXCL12 on pseudopalisading cells and proliferating microvessels in glioblastomas: an accelerated growth factor in glioblastomas. Int J Oncol 2009;34:665–72.
19. Soeda A, Park M, Lee D, Mintz A, Androutsellis-Theotokis A, McKay RD, et al. Hypoxia promotes expansion of the CD133-positive glioma stem cells through activation of HIF-1alpha. Oncogene 2009;28:3949–59.
20. Li Z, Bao S, Wu Q, Wang H, Eyler C, Sathornsumetee S, et al. Hypoxia-inducible factors regulate tumorigenic capacity of glioma stem cells. Cancer Cell 2009;15:501–13.
21. Aiuti A, Webb IJ, Bleul C, Springer T, Gutierrez-Ramos JC. The chemokine SDF-1 is a chemoattractant for human CD34+ hematopoietic progenitor cells and provides a new mechanism to explain the mobilization of CD34+ progenitors to peripheral blood. J Exp Med 1997;185:111–20.
22. Ma Q, Jones D, Borghesani PR, Segal RA, Nagasawa T, Kishimoto T, et al. Impaired B-lymphopoiesis, myelopoiesis, and derailed cerebellar neuron migration in CXCR4- and SDF-1-deficient mice. Proc Natl Acad Sci U S A 1998;95:9448–53.
23. Zou YR, Kottmann AH, Kuroda M, Taniuchi I, Littman DR. Function of the chemokine receptor CXCR4 in haematopoiesis and in cerebellar development. Nature 1998;393:595–9.
24. Teicher BA, Fricker SP. CXCL12 (SDF-1)/CXCR4 pathway in cancer. Clin Cancer Res 2010;16:2927–31.
25. Rubin JB, Kung AL, Klein RS, Chan JA, Sun Y, Schmidt K, et al. A small-molecule antagonist of CXCR4 inhibits intracranial growth of primary brain tumors. Proc Natl Acad Sci U S A 2003;100:13513–8.
26. Kioi M, Vogel H, Schultz G, Hoffman RM, Harsh GR, Brown JM. Inhibition of vasculogenesis, but not angiogenesis, prevents the recurrence of glioblastoma after irradiation in mice. J Clin Invest 2010;120:694–705.
27. Stevenson CB, Ehtesham M, McMillan KM, Valadez JG, Edgeworth ML, Price RR, et al. CXCR4 expression is elevated in glioblastoma multiforme and correlates with an increase in intensity and extent of peritumoral T2-weighted magnetic resonance imaging signal abnormalities. Neurosurgery 2008;63:560–9.
28. Bian XW, Yang SX, Chen JH, Ping YF, Zhou XD, Wang QL, et al. Preferential expression of chemokine receptor CXCR4 by highly malignant human gliomas and its association with poor patient survival. Neurosurgery 2007;61:570–8.
29. Ping YF, Yao XH, Jiang JY, Zhao LT, Yu SC, Jiang T, et al. The chemokine CXCL12 and its receptor CXCR4 promote glioma stem cell-mediated VEGF production and tumour angiogenesis via PI3K/AKT signalling. J Pathol 2011;224:344–54.
30. Bar EE. Glioblastoma, cancer stem cells and hypoxia. Brain Pathol 2011;21:119–29.

31. Calinescu AA, Nunez FJ, Koschmann C, Kolb BL, Lowenstein PR, Castro MG. Transposon mediated integration of plasmid DNA into the subventricular zone of neonatal mice to generate novel models of glioblastoma. J Vis Exp 2015;96.
32. Lin R, Iacovitti L. Classic and novel stem cell niches in brain homeostasis and repair. Brain Res 2015;1628:327–42.
33. Ligon KL, Alberta JA, Kho AT, Weiss J, Kwaan MR, Nutt CL, et al. The oligodendroglial lineage marker OLIG2 is universally expressed in diffuse gliomas. J Neuropathol Exp Neurol 2004;63:499–509.
34. Wiesner SM, Decker SA, Larson JD, Ericson K, Forster C, Gallardo JL, et al. De novo induction of genetically engineered brain tumors in mice using plasmid DNA. Cancer Res 2009;69:431–9.
35. Ding L, Morrison SJ. Haematopoietic stem cells and early lymphoid progenitors occupy distinct bone marrow niches. Nature 2013;495:231–5.
36. Lathia JD, Mack SC, Mulkearns-Hubert EE, Valentim CL, Rich JN. Cancer stem cells in glioblastoma. Genes Dev 2015;29:1203–17.
37. Koschmann C, Calinescu AA, Nunez FJ, Mackay A, Fazal-Salom J, Thomas D, et al. ATRX loss promotes tumor growth and impairs nonhomologous end joining DNA repair in glioma. Sci Transl Med 2016;8:328ra28.
38. Uchida N, Buck DW, He D, Reitsma MJ, Masek M, Phan TV, et al. Direct isolation of human central nervous system stem cells. Proc Natl Acad Sci U S A 2000;97:14720–5.
39. Spassky N, Merkle FT, Flames N, Tramontin AD, Garcia-Verdugo JM, Alvarez-Buylla A. Adult ependymal cells are postmitotic and are derived from radial glial cells during embryogenesis. J Neurosci 2005;25:10–8.
40. Gilbertson RJ, Rich JN. Making a tumour's bed: glioblastoma stem cells and the vascular niche. Nat Rev Cancer 2007;7:733–6.
41. Ausman JI, Shapiro WR, Rall DP. Studies on the chemotherapy of experimental brain tumors: development of an experimental model. Cancer Res 1970;30:2394–400.
42. McGrath KE, Koniski AD, Maltby KM, McGann JK, Palis J. Embryonic expression and function of the chemokine SDF-1 and its receptor, CXCR4. Dev Biol 1999;213:442–56.
43. Balabanian K, Lagane B, Infantino S, Chow KY, Harriague J, Moepps B, et al. The chemokine SDF-1/CXCL12 binds to and signals through the orphan receptor RDC1 in T lymphocytes. J Biol Chem 2005;280:35760–6.
44. Hattermann K, Mentlein R. An infernal trio: the chemokine CXCL12 and its receptors CXCR4 and CXCR7 in tumor biology. Ann Anat 2013;195:103–10.
45. Li M, Ransohoff RM. Multiple roles of chemokine CXCL12 in the central nervous system: a migration from immunology to neurobiology. Prog Neurobiol 2008;84:116–31.
46. Cancer Genome Atlas Research N. Comprehensive genomic characterization defines human glioblastoma genes and core pathways. Nature 2008;455:1061–8.
47. Ali SH, DeCaprio JA. Cellular transformation by SV40 large T antigen: interaction with host proteins. Semin Cancer Biol 2001;11:15–23.
48. Sidle A, Palaty C, Dirks P, Wiggan O, Kiess M, Gill RM, et al. Activity of the retinoblastoma family proteins, pRB, p107, and p130, during cellular proliferation and differentiation. Crit Rev Biochem Mol Biol 1996;31:237–71.
49. McDowell KA, Riggins GJ, Gallia GL. Targeting the AKT pathway in glioblastoma. Curr Pharm Des 2011;17:2411–20.
50. Chiariello E, Roz L, Albarosa R, Magnani I, Finocchiaro G. PTEN/MMAC1 mutations in primary glioblastomas and short-term cultures of malignant gliomas. Oncogene 1998;16:541–5.
51. Haas-Kogan D, Shalev N, Wong M, Mills G, Yount G, Stokoe D. Protein kinase B (PKB/Akt) activity is elevated in glioblastoma cells due to mutation of the tumor suppressor PTEN/MMAC. Curr Biol 1998;8:1195–8.
52. Mao W, Yi X, Qin J, Tian M, Jin G. CXCL12 inhibits cortical neuron apoptosis by increasing the ratio of Bcl-2/Bax after traumatic brain injury. Int J Neurosci 2014;124:281–90.
53. Hetschko H, Voss V, Horn S, Seifert V, Prehn JH, Kogel D. Pharmacological inhibition of Bcl-2 family members reactivates TRAIL-induced apoptosis in malignant glioma. J Neurooncol 2008;86:265–72.
54. Tabatabai G, Bahr O, Mohle R, Eyupoglu IY, Boehmler AM, Wischhusen J, et al. Lessons from the bone marrow: how malignant glioma cells attract adult haematopoietic progenitor cells. Brain 2005;128:2200–11.
55. Martini F, Iaccheri L, Lazzarin L, Carinci P, Corallini A, Gerosa M, et al. SV40 early region and large T antigen in human brain tumors, peripheral blood cells, and sperm fluids from healthy individuals. Cancer Res 1996;56:4820–5.
56. Suzuki SO, Mizoguchi M, Iwaki T. Detection of SV40 T antigen genome in human gliomas. Brain Tumor Pathol 1997;14:125–9.
57. Holland EC, Celestino J, Dai C, Schaefer L, Sawaya RE, Fuller GN. Combined activation of Ras and Akt in neural progenitors induces glioblastoma formation in mice. Nat Genet 2000;25:55–7.
58. Marumoto T, Tashiro A, Friedmann-Morvinski D, Scadeng M, Soda Y, Gage FH, et al. Development of a novel mouse glioma model using lentiviral vectors. Nat Med 2009;15:110–6.
59. de Vries NA, Bruggeman SW, Hulsman D, de Vries HI, Zevenhoven J, Buckle T, et al. Rapid and robust transgenic high-grade glioma mouse models for therapy intervention studies. Clin Cancer Res 2010;16:3431–41.
60. deCarvalho AC, Nelson K, Lemke N, Lehman NL, Arbab AS, Kalkanis S, et al. Gliosarcoma stem cells undergo glial and mesenchymal differentiation in vivo. Stem Cells 2010;28:181–90.
61. Mo W, Chen J, Patel A, Zhang L, Chau V, Li Y, et al. CXCR4/CXCL12 mediate autocrine cell- cycle progression in NF1-associated malignant peripheral nerve sheath tumors. Cell 2013;152:1077–90.
62. Bhardwaj A, Srivastava SK, Singh S, Arora S, Tyagi N, Andrews J, et al. CXCL12/CXCR4 signaling counteracts docetaxel-induced microtubule stabilization via p21-activated kinase 4-dependent activation of LIM domain kinase 1. Oncotarget 2014;5:11490–500.
63. Nance E, Zhang C, Shih TY, Xu Q, Schuster BS, Hanes J. Brain-penetrating nanoparticles improve paclitaxel efficacy in malignant glioma following local administration. ACS Nano 2014;8:10655–64.
64. Burkhart DL, Sage J. Cellular mechanisms of tumour suppression by the retinoblastoma gene. Nat Rev Cancer 2008;8:671–82.
65. Khan MZ, Brandimarti R, Shimizu S, Nicolai J, Crowe E, Meucci O. The chemokine CXCL12 promotes survival of postmitotic neurons by regulating Rb protein. Cell Death Differ 2008;15:1663–72.
66. Wiedemeyer WR, Dunn IF, Quayle SN, Zhang J, Chheda MG, Dunn GP, et al. Pattern of retinoblastoma pathway inactivation dictates response to CDK4/6 inhibition in GBM. Proc Natl Acad Sci U S A 2010;107:11501–6.
67. Heddleston JM, Li Z, McLendon RE, Hjelmeland AB, Rich JN. The hypoxic microenvironment maintains glioblastoma stem cells and promotes reprogramming towards a cancer stem cell phenotype. Cell Cycle 2009;8:3274–84.